

# We are IntechOpen, the world's leading publisher of Open Access books Built by scientists, for scientists

6,900

Open access books available

185,000

International authors and editors

200M

Downloads

Our authors are among the

154

Countries delivered to

TOP 1%

most cited scientists

12.2%

Contributors from top 500 universities



WEB OF SCIENCE™

Selection of our books indexed in the Book Citation Index  
in Web of Science™ Core Collection (BKCI)

Interested in publishing with us?  
Contact [book.department@intechopen.com](mailto:book.department@intechopen.com)

Numbers displayed above are based on latest data collected.  
For more information visit [www.intechopen.com](http://www.intechopen.com)



# New Results in the Theory and Practical Application of Color

*Mikhail Dolomatov*

## Abstract

The chapter provides new data on color phenomenon that we have discovered in recent years for complex and simple substances. For example, these are the effects of the relationship of physical and chemical properties and color characteristics (in color systems RGB or XYZ) of compounds (color properties principle). In particular, the effects of conjugation of ionization potential and electron affinity of light-absorbing molecules in the visible region were found. The theoretical explanation of these effects from the position of quantum theory is given. Using mathematical statistics, it is shown that the effects can be used for practical measurement of various properties of complex multicomponent substances. The results indicate the practical use of these effects in chemical technology, nanophysics, and clinical medicine.

**Keywords:** absorption spectrum, color characteristics, color systems, RGB, XYZ, physical properties, chemical properties, quantum theory, spectra of blood

## 1. Introduction

Even the Arab alchemists, the first chemists of the seventeenth and eighteenth centuries, talked about the relationship between color change and changes in the physical properties of various substances [1]. For example, the temperature of substances and their chemical transformations were estimated approximately by color. Here, new data on color phenomenon that we have discovered in recent years for complex and simple substances is provided. For example, these are the effects of the relationship of physical and chemical properties and color characteristics of compounds ("color properties principle") [2–10]. Color characteristics were measured by standard methods in colorimetric systems RGB or XYZ [11–13]. In particular, the effects of the relationship between the vertical ionization potentials and the electron affinity of light-absorbing molecules in the visible region were found [14–18]. The results indicate the practical use of these effects in chemical technology and nanophysics. We assume that the cause of these phenomena is quantum entanglement and strong correlation of electron states [19]. We established new physical effects between spectral densities (integral absorption, reflection, and transmission characteristics) with ionization potential and electron affinity [2–4, 15, 18–21]. We propose to use these effects in determining the energies of electronic states. Methods for determination of IP and EA for molecules and organic semiconductors have been developed. We propose to use these effects in determining the energies of electronic states. In addition, the color characteristics of biological fluids were

investigated. In addition, we have determined the averaged color characteristics of the electromagnetic spectrum for aqueous solutions of hemolyzed blood, plasma, and serum from 100 donors and 95 patients with different diagnoses and different severities of their conditions. From the averaged absorption spectra, we calculated the color characteristics of the hemolyzed blood, plasma, and serum from the donors and patients by the standard CIE procedure. The blood is considered as a single, indivisible light-absorbing system in studying complex biological specimens. We studied the relationship between the color characteristics of human blood in normal and pathological conditions [22–26]. Let us consider these aspects in more detail.

## 2. Estimation of physicochemical properties of complex systems according to color characteristics

We have discovered new optical effects of the relationship between the physicochemical properties and color characteristics for very complex chemical systems [2–4]. In particular, the dependencies between the properties and color characteristics of multicomponent hydrocarbon systems are investigated. Dependencies between color coordinates (luminosity) and various physical and chemical characteristics of these substances are established. All results are confirmed by statistical data processing. The dependence of the properties on the CCs is linear (the law “color-properties”):

$$Z = B_0 + B_1 \cdot q \quad (1)$$

where  $Z$  is one of the physical or chemical properties,  $q$  is the one of the color characteristics of the substance (e.g., color coordinates  $X_j, Y_j, Z_j$  in the XYZ system or  $R_j, G_j, B_j$  in the RGB system; or chromaticity coordinates  $x_j, y_j, z_j$  in the XYZ system or trichromatic coordinates  $r_j, g_j, b_j$  in the RGB system;  $j$ , standard light source A, B, C, or D), and  $B_0, B_1$  are the empirical constants dependent on the type of the source and the class of researched substances and dimensional properties.

Color coordinates of  $(X, Y, Z)$ , coordinates of chromaticity  $(x, y, z)$ , hue  $(\lambda)$ , and luminosity  $(L)$  have been taken as color characteristics [11–13]. CCs of multicomponent hydrocarbonic systems have been determined by the technique of the International Committee on Illumination (Commission Internationale de l’Eclairage, CIE) [11] for four standard sources (illuminants) A, B, C, and  $D_{65}$ . The technique, corrected for optically transparent [13] medium, has been used. Electron absorption spectra of multicomponent hydrocarbon systems have been determined in toluene solutions in the range of 380–780 nm with the use of automatic spectrophotometer.

The CCs were defined on the methods CIE [12, 13] in the revised version to optical transparent solutions via the transparent coefficients— $\tau(\lambda)$ . The color properties were calculated from formulas (2)–(7):

$$\begin{aligned} X &= \sum_{380}^{780} E(\lambda) \tau(\lambda) \bar{x}(\lambda) \Delta\lambda \\ Y &= \sum_{380}^{780} E(\lambda) \tau(\lambda) \bar{y}(\lambda) \Delta\lambda \\ Z &= \sum_{380}^{780} E(\lambda) \tau(\lambda) \bar{z}(\lambda) \Delta\lambda \end{aligned} \quad (2)$$

where  $X$ ,  $Y$ , and  $Z$  are the tristimulus values for system CIE;  $E(\lambda)$  is the spectral power distribution for the spectrum of emission source;  $\bar{x}$ ,  $\bar{y}$ , and  $\bar{z}$  are three color-matching functions CIEXYZ; and  $\tau(\lambda)$  is the spectral function of transparent coefficients in the visible region.

The transparent coefficient is defined on known relationships:

$$\tau(\lambda) = 10^{-c \cdot k(\lambda)} \quad (3)$$

$k(\lambda)$ —absorption coefficient.

$$k(\lambda) = D/cL \quad (4)$$

where  $D$  is the optical density of solutions,  $c$  is the concentration, and  $L$  is the thickness of absorption layer.

For more hydrocarbon systems, the solutions were prepared with concentration near 0.002 g/l; similarly, as in this case, we got the result with minimal errors.

The relations for  $X$ ,  $Y$ ,  $Z$  are presented in matrix form [12]:

$$\begin{pmatrix} X \\ Y \\ Z \end{pmatrix} = \begin{pmatrix} E(\lambda_1)\bar{x}(\lambda_1) & E(\lambda_2)\bar{x}(\lambda_2) & \dots & E(\lambda_i)\bar{x}(\lambda_i) \\ E(\lambda_1)\bar{y}(\lambda_1) & E(\lambda_2)\bar{y}(\lambda_2) & \dots & E(\lambda_i)\bar{y}(\lambda_i) \\ E(\lambda_1)\bar{z}(\lambda_1) & E(\lambda_2)\bar{z}(\lambda_2) & \dots & E(\lambda_i)\bar{z}(\lambda_i) \end{pmatrix} \begin{pmatrix} \tau(\lambda_1) \\ \tau(\lambda_2) \\ \dots \\ \tau(\lambda_{i-1}) \\ \tau(\lambda_i) \end{pmatrix} \quad (5)$$

$$\Phi_{XYZ} = E_{XYZ} \cdot T \quad (6)$$

where  $\Phi_{XYZ}$  is the column vector of color coordinates for objects of investigation in the system XYZ,  $E_{XYZ}$  is the product matrix of spectral power distribution for standard source and three color-matching functions, and  $T$  is the column vector for coefficient of transparency.

The chromaticity coordinates were calculated on formulas in the system CIE (12).

$$x = \frac{X}{X+Y+Z}, \quad y = \frac{Y}{X+Y+Z}, \quad z = \frac{Z}{X+Y+Z} \quad (7)$$

where  $x$ ,  $y$ , and  $z$  are chromaticity coordinates.

In **Table 1** the defined CCs of multicomponent petrochemical systems are given [3, 4]. As it can be seen from the results of the calculations, CCs at the identical radiation source are close among themselves despite their different nature. Obviously, the reason of similarity of color properties is the similarity of the absorption spectra of the systems researched. Also the research has shown that multicomponent petrochemical systems do not have color isomerism, i.e., their CCs change depending on the radiation sources.

The coefficients  $B_0$  and  $B_1$  Eq. (1) have been calculated by the method of least squares. As the criterion of adequacy, the correlation coefficient  $R$  and the mean-square deviation have been taken. Some results of the calculations are given in **Table 2**. The received results show that for all the researched petrochemical systems, there is correlation dependence PCP from CCs [2–4].

In many processes, it is necessary to take express control of the PCPs. Therefore, the dynamic form of Eq. (8) has been investigated in the author's very last investigation of more than 300 of multicomponent hydrocarbon systems:

$$\Delta Z_k = b \cdot \Delta q_k \quad (8)$$

Hydrocarbon systems	CIE standard source	Luminosity	Coordinates of chromaticity		
			x	y	z
Separator oils of the Russian Federation (Bashkortostan, West Siberia, Tatarstan)	A	20.56–70.59	0.51–0.63	0.36–0.42	0.00–0.08
	B	17.24–66.60	0.39–0.51	0.42–0.49	0.00–0.19
	C	15.73–65.91	0.38–0.54	0.38–0.47	0.01–0.24
	D <sub>65</sub>	17.17–67.42	0.37–0.51	0.39–0.50	0.01–0.23
Blown, residual, road, and structural petroleum	A	9.80–64.97	0.51–0.67	0.32–0.42	0.00–0.07
	B	7.76–61.44	0.40–0.55	0.44–0.46	0.01–0.16
	C	6.60–60.88	0.38–0.61	0.38–0.43	0.02–0.22
	D <sub>65</sub>	7.48–62.79	0.38–0.57	0.41–0.45	0.01–0.21
Organic fractions of oligomers	A	68.23–87.09	0.50–0.52	0.39–0.40	0.08–0.11
	B	64.75–84.41	0.36–0.38	0.39–0.41	0.20–0.25
	C	64.40–84.71	0.34–0.37	0.35–0.37	0.26–0.32
	D <sub>65</sub>	65.66–85.51	0.34–0.37	0.36–0.39	0.25–0.30
Residual high-boiling hydrocarbonic fraction of vacuum oil refining	A	15.26–86.19	0.51–0.66	0.33–0.40	0.00–0.09
	B	12.15–82.06	0.38–0.57	0.42–0.47	0.01–0.20
	C	10.41–81.90	0.36–0.62	0.36–0.44	0.01–0.26
	D <sub>65</sub>	11.80–83.30	0.36–0.58	0.39–0.46	0.01–0.25
Hydrocarbonic fractions with average boiling temperature T <sub>boil</sub> 180–360°C	A	21.20–99.83	0.48–0.63	0.36–0.41	0.01–0.14
	B	17.70–98.97	0.33–0.52	0.36–0.48	0.03–0.30
	C	15.98–99.96	0.31–0.55	0.32–0.45	0.04–0.37
	D <sub>65</sub>	17.57–99.90	0.31–0.52	0.33–0.47	0.04–0.36
Asphaltenes and tars	A	0.10–98.67	0.29–0.86	0.14–0.41	0.00–0.33
	B	0.09–97.66	0.04–0.62	0.32–0.64	0.00–0.32
	C	0.08–98.67	0.04–0.71	0.24–0.59	0.00–0.37

**Table 1.**  
*Range of color characteristics of multicomponent hydrocarbon systems [3, 4].*

where  $\Delta Z$  is the change of the physicochemical property and  $\Delta q$  is the change of CCs. Eq. (8) means that a change of properties is proportional to the change of color for any colored substances.

The received results show that for all the researched petrochemical systems, there is correlation dependence PCP from CCs. The correlation coefficient R and the standard deviation were used as the criterion of adequacy. Some results of calculations are given in **Table 2**. Properties such as relative density ( $\rho$ ); number-average molecular weight (M in Dalton); Conradson carbon residue (g in weight.%); activation energy for viscous flow (Ea in kJ/mol). The results show that for all studied petrochemical systems, there is a clear dependence of PCP on CCs [2–4]. These correlations allow the determination of PCP substances using CCs. Such dependencies are necessary for quality control of oil distillates and oil products. In addition, there is an opportunity for remote control methods of environmental pollution by oil and oil products.

For example, it is possible to determine in a few minutes such properties of formation oils as molecular mass, viscosity, density, the index of thermal stability, the index of reactivity of fractions in coking, thermal cracking processes, etc.

Multicomponent hydrocarbon system	PCP	CC	Coefficients of Eq. (1)		Correlation coefficient	Variation coefficient (%)	Fisher's ratio test for sample volume F
			B <sub>0</sub>	B <sub>1</sub>			
Raw oils	p	y <sub>D</sub>	0.793	0.349	0.98	0.05	887.80
		g <sub>A</sub>	0.758	0.310	0.98	0.05	889.46
	M	X <sub>A</sub>	846.429	−4.563	0.99	0.48	1931.49
		R <sub>A</sub>	897.646	−2.683	0.99	0.46	2084.20
	g	Y <sub>B</sub>	17.063	−0.150	0.96	3.23	453.22
		R <sub>C</sub>	17.984	−0.098	0.96	3.20	460.43
	Ea	Y <sub>B</sub>	37.701	−0.376	0.97	5.17	536.05
		G <sub>A</sub>	37.463	−0.140	0.97	5.16	536.51
Petroleum residues	p	x <sub>C</sub>	0.757	0.462	0.99	0.27	577.35
		r <sub>C</sub>	0.874	0.240	0.99	0.20	1019.05
	M	Y <sub>B</sub>	877.611	−6.183	0.95	4.50	146.34
		r <sub>A</sub>	−121.96	1157.340	0.96	4.31	161.29
	g	x <sub>D</sub>	−34.205	106.697	0.98	6.80	341.48
		r <sub>C</sub>	−6.530	53.960	0.98	5.92	455.11
	Ea	x <sub>D</sub>	−76.698	228.968	0.98	8.31	308.21
		r <sub>B</sub>	−22.755	110.594	0.98	7.53	378.34
Bitumens and bituminous materials	p	x <sub>D</sub>	0.612	0.676	0.98	0.26	260.20
		r <sub>C</sub>	0.876	0.209	0.99	0.22	384.50
	M	X <sub>A</sub>	−11.918	1308.245	0.99	1.61	797.32
		R <sub>A</sub>	1341.792	−6.249	0.99	1.47	958.95
	g	y <sub>A</sub>	−570.815	255.283	0.98	3.62	252.80
		g <sub>A</sub>	241.685	−379.399	0.98	3.64	249.38
	Ea	Y <sub>A</sub>	−0.878	68.000	0.98	3.32	294.90
		G <sub>A</sub>	64.355	−0.341	0.98	3.36	287.60

\* $\rho$  = relative density; M = number-average molecular weight, moles; g = Conradson carbon residue, wt.%; Ea = activation energy for viscous flow, kJ/mol.

**Table 2.**  
Coefficients of Eq. (10) for physicochemical property estimation of oils and petroleum residues in colorimetric systems XYZ and RGB [3–10].

### 3. Introduction of electronic phenomenological spectroscopy

The method of electronic phenomenological spectroscopy (EPS) was first proposed by Mikhail Dolomatov [2, 3]. In recent years, this science direction has been intensively developed by the Dolomatov group at the Oil Technical State University and Bashkir State University (Ufa) in Russia. There are the following approaches and physical phenomena in the basis of EPS:

Unlike conventional spectroscopic methods, the EPS studies substances as a comprehensive quantum quasicontinuum without separating the spectrum of the substance into characteristic spectral bands by certain resonance frequencies or wavelengths of individual functional groups or components. The spectrum is



studied as a single system (broadband signal) from a set of electronic states. Therefore, at this system integral level, there are new physical effects, not previously known. For example, the effects of the relationship of integral optical characteristics with different macroscopic and quantum properties of the substance as a whole by quantum quasicontinuum “spectrum-properties” and “color-properties” are observed. Qualitatively new physical phenomena appear when considering systems interacting with radiation in a wide optical spectrum. According to these laws, changes in the physical and chemical properties of substances cause a change in the integral characteristics of absorbed, reflected, or emitted radiation in the ultraviolet (UV), visible, and near-infrared (IR) regions of the electromagnetic spectrum. This allows the use of EPS methods for the study of individual and complex multicomponent substances.

For example, there may be a relationship between the integral force of the oscillator and some physical and chemical properties Z:

$$\Delta Z = c \cdot \Delta \theta \quad (9)$$

Here  $\theta$  is the integral absorption—integral oscillator force (IOF), which has a simple physical explanation, namely, the area under the radiation absorption curve for the visible and UV regions of the spectrum,  $l \text{ nm mole}^{-1} \text{ cm}^{-1}$ ;

$c$  is the constant depending on the method of measuring the spectrum, the nature of the substance, and individual for each property.

Therefore, it can be assumed that there is a relationship between any integral optical characteristic of a wide-spectrum signal (**Figure 4**) and properties having the form.

$$\Delta Z = c \cdot \Delta P \quad (10)$$

Here,  $P$  is the integral spectral parameter, for example, integrated oscillator power, color characteristics, integral autocorrelation function, or relative imperial parameter and others into **Figure 1**.

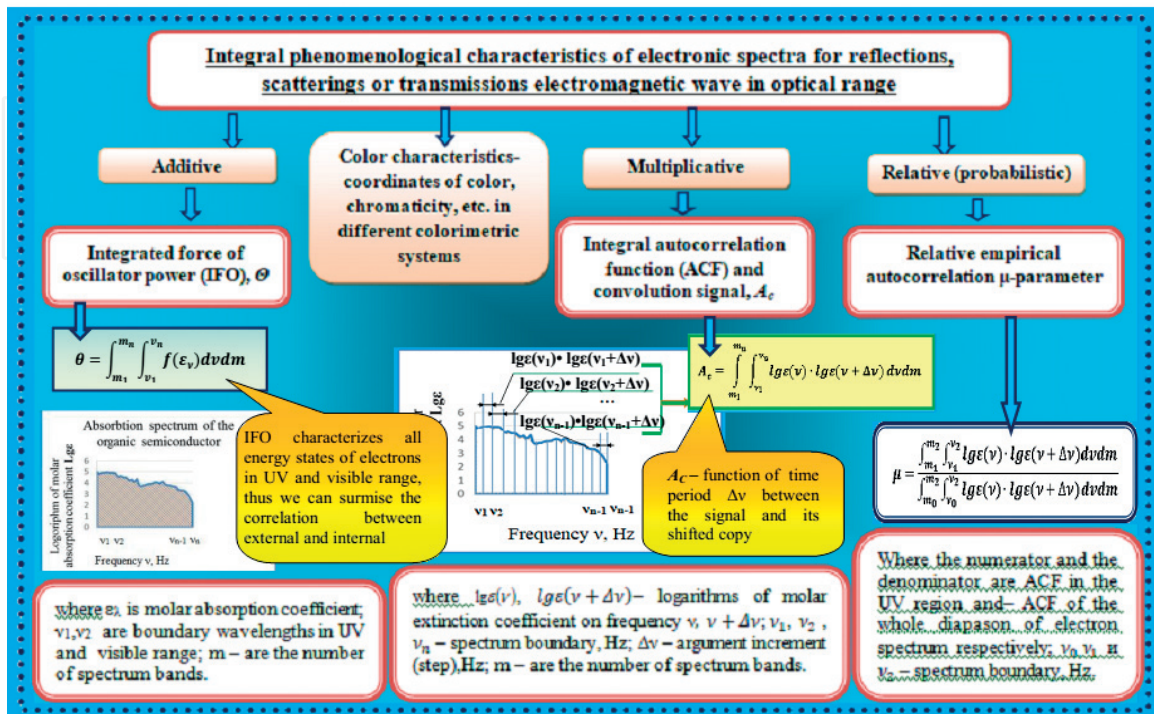


**Figure 1.**  
Integral phenomenological characteristics of electronic spectra.

Obviously, a special case of Eq. (10) is the effect of “color-properties” (1) (we found with the coauthors O. Kydyrgychova, L. Dolomatova and V. Kartasheva in 1999 [5]). Phenomenological spectroscopy methods have been developed for identification and simultaneous determination of a set of different physical and chemical properties of natural and technical multicomponent organic systems, as well as properties of individual substances. For example, in a few minutes, it is possible to determine such properties of formation oils as the average molecular weight, viscosity, density, thermal stability index, index of reactivity of fractions in the processes of coking and thermal cracking, etc. EPS methods were adopted in the oil and petrochemical industry [2–4], environmental monitoring [3], biophysics and medicine [24, 25], nanotechnology and molecular electronics [15–18], and space exploration.

For science and technology, of interest are laws of the relationship of the integral characteristics of the spectrum and the electronic properties of matter. The knowledge of the electron structure of the molecular substances and materials has the fundamental importance for solving real problems in many fields of science and technology (physic of solid state, chemistry, electronics, electrical engineering). Despite progress in the experimental and quantum methods in some cases, there are significant discrepancies between the predicted values and experimental results of electron structure determination of complex materials and compounds. Many compounds and some materials for nanotechnology are characterized by complex structure and chemical and phase instabilities. Therefore, it is necessary to create new methods for assessing electronic structures, for example, ionization potentials, affinities to electron, and some other properties.

Hence the difficulty of determining the first ionization potentials (IP), the affinity of electrons (EA) and other characteristics of the energies of electronic states for such systems.

As known, ionization energy is the energy required to remove an electron from an atom or molecule. The unit of measurement of this physical quantity is the amount of energy required to remove one electron from one atom or molecule, expressed in electronic volts. The ionization potential (IP) is the electrical potential at which an electron leaves an atom or molecule, overcoming the forces of attraction. This process forms a positive ion [27, 28].



If during the electronic transition the geometry of the molecule changes minimally, it is said about the vertical IP. Next, we will consider the vertical potential only. According to the theorem of Koopmans, the first vertical ionization energy of a molecular system is equal to the negative of the orbital energy of the highest occupied molecular orbital (HOMO).

The electron affinity (EA) of an atom or molecule is defined as the amount of energy released or spent when an electron is added to a neutral atom or molecule with the formation of a negative ion [28].



In the chemistry IP and EA are the characteristics for ability of molecules to donor-acceptor properties [27]. These physical values may be used for the determination of the indexes of reactivity of molecules (a characteristic of its chemical activity).

In previous works [2, 14, 20, 21], we established new physical effects between spectral densities (integral absorption, reflection, and transmission characteristics)



with IP and EA. We propose to use these effects in determining the energies of electronic states. Methods for determination of IP and EA for molecules and organic semiconductors have been developed. We propose to use these effects in determining the energies of electronic states.

The IP and the EA of materials were estimated from the empirical dependencies linking these characteristics with the integral parameter of UV and/or vis spectrum:

$$E = \alpha_0 + \alpha_1 P \quad (13)$$

where  $E$  is effective ionization potential or effective electron affinity, eV;  $\alpha_1$  and  $\alpha_2$  are empirically determined coefficients, and  $P$  is the integral spectral parameter. For example, integrated oscillator force (IOF), color characteristics, integral auto-correlation function or relative empirical parameter, and others (**Figure 1**).

The first experiments in the detection of the phenomenon (2) were carried out in 1988–1992 together with the Dr. G. Mukaeva [14]. The dependence of IP and EA on the integral oscillator force (IOF) was established by the results of the study of about 200 optical spectra of atoms and organic molecules:

$$E = \alpha_1 + \alpha_2 \cdot \theta, \quad (14)$$

Integral spectral characteristic can be any physical value of general absorption or emission of electromagnetic radiation, such as integral oscillator force (IOF):

$$\theta = \int_{\delta} \int_{\xi} f(\xi) d\xi d\delta \quad (15)$$

where  $\theta$  is a reflection of quantum continuum as the sum of different states of electron, for example, all vibration states and electron states of transition among different levels,  $f(\xi)$  is spectral function of absorption or emission of radiation, and  $\delta$  is a range of resonance wavelengths or frequencies.

Let us consider the method, which was proved in our previous works [14, 15]. The IP and EA are estimated according to empirical dependencies which link these characteristics with logarithmic integral index of absorption (1).

$$E = \alpha_1 + \alpha_2 \theta_{lg}, \quad (16)$$

Here  $E$  is the ionization potential or an electron affinity, eV;  $\alpha_1$  and  $\alpha_2$  are empirically determined coefficients, eV and eV · nm<sup>-1</sup>, respectively.

$$\int_{\lambda_1}^{\lambda_2} \lg \varepsilon_{\lambda} d\lambda = \theta_{lg} \quad (17)$$

where  $\varepsilon(\lambda)$  is the molar extinction coefficient, l mol<sup>-1</sup> cm<sup>-1</sup>;  $\theta_{lg}$  is the integral logarithmic index of absorption (logarithmic IOS), ·nm;  $\lambda_1$  and  $\lambda_2$  are borders of the spectrum in UV and (or) visible region, nm; and  $\lambda_1$  and  $\lambda_2$  are the borders of wavelength of the spectrum in UV and (or) visible region.

**Table 3** shows the corresponding coefficients for the dependencies (16) in different classes of organic molecules.

Breakthrough research in this area was done in collaboration with Dr. D. Shulyakovskii, Dr. E. Kovaleva, Dr. G. Yarmuhamedova, N. Paimurzina, and K. Latypov [20, 21]. We established the following regularities, which connected the integral parameters of the spectrum with IP and EA (18)–(21).

Dependence		$E = \alpha_1 + \alpha_2 \cdot \theta_{lg}$				
Homologous series	IP or EA	Coefficient of correlation equations		Statistic characteristics		
		$\alpha_1$ , eV	$\alpha_2, 10^{-7}$ eV nm <sup>-1</sup>	Correlation coefficient	Mean-square deviation, eV	Variation coefficient, %
Polycyclic aromatic compounds	IP	8.074	-0.0010256	0.76	0.22	3.07
Polycyclic aromatic compounds	EA	0.290	0.00064502	0.71	0.16	2.22
Nitrogen-containing compounds [35]	IP	10.11	-0.00250000	0.88	0.26	2.46
Oxygen-containing compounds [35]	IP	11.03	-0.00347000	0.82	0.32	2.54

**Table 3.**  
Coefficients of dependence (16) for homologous series.

$$IP = \gamma_1 + \gamma_2 \cdot A_{Cv}, \tag{18}$$

$$EA = \chi_1 + \chi_2 \cdot A_{Cv}, \tag{19}$$

$$IP = \varphi_1 + \varphi_2 \cdot \mu, \tag{20}$$

$$EA = \eta_1 + \eta_2 \cdot \mu, \tag{21}$$

IP is the effective ionization potential; EA is the effective electron affinity;  $A_{Cv}$  is integral autocorrelation function of the electron spectrum (IAFS) (23);  $\mu$  is the relative empirical autocorrelation parameter ( $\mu$ , parameter) (24);  $\varepsilon(\nu)$  is the density distribution function of the radiation absorption;  $\nu$  is the spectral frequency;  $\gamma_0$ ,  $\gamma_1$ ,  $\chi_1$ ,  $\chi_2$ ,  $\eta_1$ ,  $\eta_2$ ,  $\varphi_0$ , and  $\varphi_1$  are empirically defined coefficients (Table 4); and  $m$  is the number of spectrum bands.

In the calculation of integral parameters using the autocorrelation function of the signal, we have used the techniques adopted in statistical physics and spectroscopy [29]. We presented the energy spectrum of the molecule in the form of the integral of the autocorrelation function (IACF), frequency-dependent transitions. The integral autocorrelation function (ACF) is defined by the following formula:

Group of organic semiconductor	Constants by (18) and (19) eV		Constants by (18) and (19), 10 <sup>-17</sup> eV s		Determination coefficient, R <sup>2</sup>	
	$\gamma_1$	$\chi_1$	$\gamma_2$	$\chi_2$	IP	EA
Complex oxy-compounds	9.35	0.08	-1.96	1.24	0.90	0.88
Ketones and aldehydes	10.65	-0.02	-2.98	1.76	0.85	0.81
Constants by (20) and (21), eV					Determination coefficient, R <sup>2</sup>	
Polycyclic aromatic hydrocarbons	$\varphi_1$	$\varphi_2$	$\eta_1$	$\eta_2$	IP	EA
	5.43	1.68	1.88	-1.36	0.88	0.87

**Table 4.**  
Constants and determination coefficients for dependencies (14–16).

$$A(\Delta\omega) = \int_{\omega_0}^{\omega_2} f(\omega)f(\omega + \Delta\omega)d\omega \quad (22)$$

where  $\omega = 2\pi\nu$ , cyclical frequency,  $s^{-1}$ .

In [20] we proposed numerical parameter from IACP in the optical spectra was determined with the logarithmic function. The parameters of the ACF are because numbers are calculated using definite integral.

$$A_\nu = \int_{m_1}^{m_2} \int_{\nu_1}^{\nu_2} \epsilon(\nu)\epsilon(\nu + \Delta\nu)d\nu dm \quad (23)$$

where  $\lg\epsilon(\nu)$  and  $\lg\epsilon(\nu + \Delta\nu)$  are logarithms of molar extinction coefficient on frequency  $\nu$ ,  $\nu + \Delta\nu$ ;  $\nu_1$ ,  $\nu_2$ , and  $\nu_n$  are the spectrum boundary, Hz;  $\Delta\nu$  is the argument increment (step), Hz; and  $m$  is the number of spectrum bands.

$$\mu = \frac{\int_{m_1}^{m_2} \int_{\nu_1}^{\nu_2} \lg\epsilon(\nu) \cdot \lg\epsilon(\nu + \Delta\nu)d\nu dm}{\int_{m_0}^{m_2} \int_{\nu_0}^{\nu_2} \lg\epsilon(\nu) \cdot \lg\epsilon(\nu + \Delta\nu)d\nu dm} \quad (24)$$

where the numerator of fraction is the integral autocorrelation function (IACF) in the UV spectral region; the denominator is IACF in the UV-vis spectral region;  $\nu$ ,  $\nu + \Delta\nu$ ;  $\nu_1$ ,  $\nu_2$ , and  $\nu_n$  are the spectrum boundary  $10^{14}$  Hz;  $\Delta\nu$  is small increment of the argument (the analysis step of  $1.5 \times 10^{16}$  Hz);  $\lg\epsilon(\nu)$  and  $\lg\epsilon(\nu + \Delta\nu)$  are molar absorption coefficients at certain frequencies; and  $m$  is the number of spectrum bands.

The dependencies of IP and EA on the  $\mu$ -factor for polycyclic aromatic hydrocarbons (PAH) of various classes (**Figures 2 and 3**) are established [20]. In addition, the dependencies of IP and EA on IACP for oxygen-containing compounds (alcohols, aldehydes, ketones) (**Figures 4 and 5**) are established [21].

IP and EA of organic molecules and PAH of different origin are presented in **Tables 5 and 6**.

EA and IP of organic molecules and semiconductors of different origins are presented in **Tables 2 and 3**.

Thus it is established that IP and EA of PAH, calculated by RHF 6-31G\*\* and DFT methods, have the IACF dependence and  $\mu$ -factor. These dependencies allow

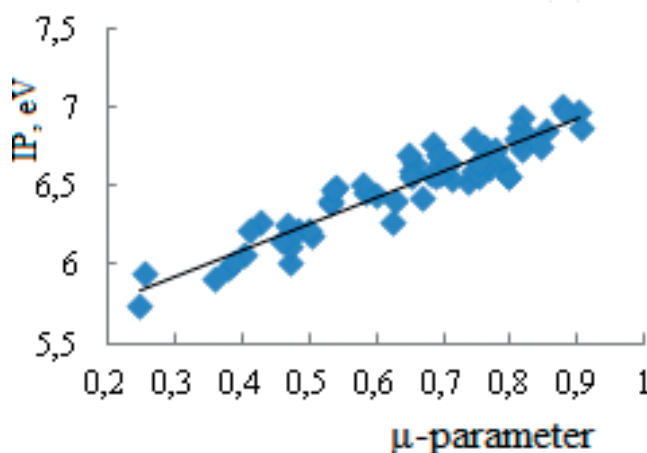


**Figure 2.**  
Relationship of IP with the relative empirical autocorrelation parameter  $\mu$  for PAH.

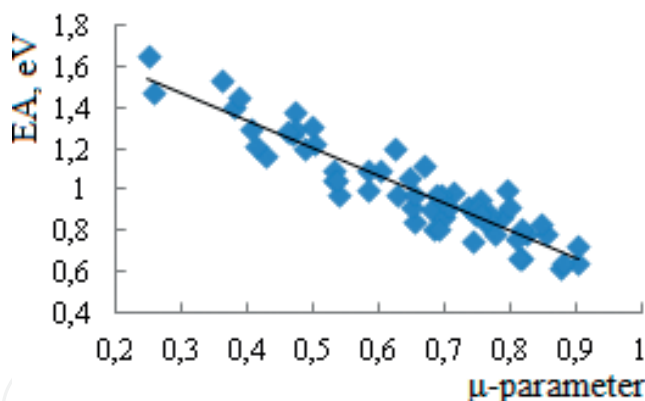


**Figure 3.**  
 Relationship of EA with the relative empirical autocorrelation parameter  $\mu$  for PAH.

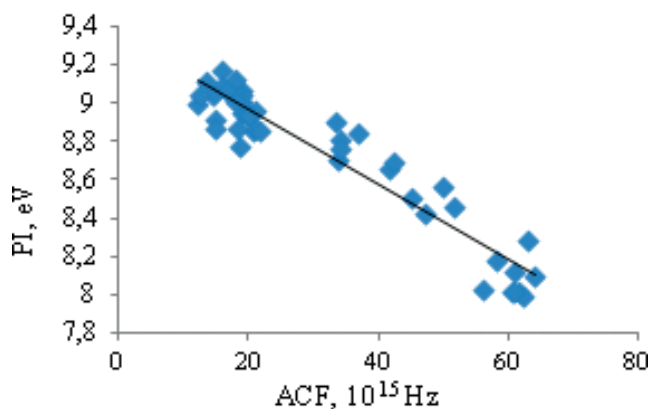


**Figure 4.**  
 Relationship of IP from IACF of organic oxygen groups containing molecules.

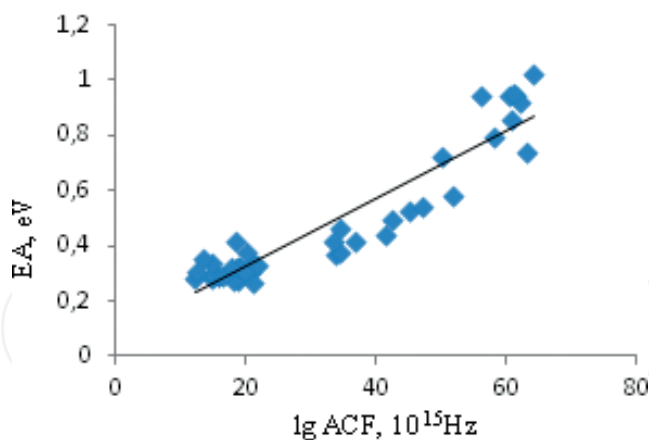


**Figure 5.**  
 Relationship of EA from IACF of organic oxygen groups containing molecules.

simplification of the estimations of IP and EA of organic molecules and PAH of different origin (**Tables 5 and 6**).

Thus, new methods for determining characteristics of electronic structure of different molecules and organic semiconductors are developed.

Subsequently, dependence (14) was confirmed by the study of IP and EA for various classes of sulfur and nitrogen organic compounds, organic dyes, amino acids, and biological fluids [24].

In studies [2–4] for very complex multicomponent systems, the problem of determining the electronic structure and, consequently, chemical activity was solved.

Molecules	$\mu$ - parameter	IP method DFT, eV	IP Eq. (4), eV	EA method DFT, eV	EA Eq. (5), eV
Hexahelicene	0.900	6.97	6.94	0.64	0.66
1,2,3,4,7,8-Tribenzotetracene	0.820	6.82	6.81	0.78	0.77
Heptaphene	0.745	6.60	6.68	0.88	0.87
Pentacene	0.404	6.07	6.10	1.30	1.33
1,2-Benzpentacene	0.503	6.18	6.27	1.23	1.20
1,2-3,4-8,9-10,11-Tetrabenzpentacene	0.600	6.44	6.43	1.10	1.07
Naphtho-(2'.3':3.4)-pyrene	0.647	6.70	6.52	1.06	1.00
3,4-Benznaphtho(2'',3'':8,9)-pyrene	0.472	6.12	6.71	1.30	0.84
3,4-Benznaphtho(2'',3'':9,10)-pyrene	0.531	6.41	6.20	1.05	1.26
1,14-4,5-Dibenzpentacene	0.765	6.66	6.69	0.86	0.86
1,2-Benzphenanthrene-(9',10':6,7)-pyrene	0.775	6.73	6.61	0.78	0.92
1,16-4,5-Dibenzhexacene	0.624	6.28	6.58	1.20	0.95
1,2-11,12-Dibenzperylene	0.378	5.98	6.06	1.41	1.37
1,12-2,3-Dibenzperylene	0.807	6.81	6.78	0.76	0.79
1,2-5,6-Dibenzcoronene	0.760	6.76	6.70	0.84	0.85

**Table 5.**  
*Calculated values of IP and EA.*

Molecules	ACF, $10^{15}$ Hz	IP method HF, eV	IP Eq. (2), eV	EA method HF, eV	EA Eq. (3), eV
1-Phenylacetylbutadiene	55.46	9.01	9.00	0.99	0.96
2-Furylpolyenoic acids $C_4H_3O-(CH=CH)_2COOH$	61.49	8.92	8.95	1.13	1.06
Polyenoic acid	64.39	8.77	8.87	1.11	1.10
9-Oxoacridine	41.32	8.38	8.69	1.15	1.01

**Table 6.**  
*Calculated values of IP and EA.*

The characteristics of the chemical activity can be determined from the electron absorption spectra simplification. The authors introduced new values: effective IP and effective electron affinity [30]. The effective IP and EA are the averaged potentials of ionization and the electron affinity of the radiation-absorbing components.

They allow to estimate the electron states of multicomponent and high-molecular substances, such as heavy residual resins of oil processing, high-molecular mixtures, and others.

Determining the electronic structure of materials and nanomaterials is an important problem of molecular electronics. For this, EPS was used. This application of EPS to determine the electronic structure of high-molecular compounds of petroleum (petroleum asphaltenes) was proposed in our previous works (Dolomatov et al.) [2–4, 30].



Asphaltenes	EIP, eV	EEA, eV	Band gap energy, eV	Quasi Fermi level, eV
Asphaltenes of Radevski oil	5.70	1.85	3.85	1.92
Asphaltenes of Surgut oil	5.20–5.70	2.10–2.50	3.10–3.20	1.55–1.60
Asphaltenes of distillate fraction	4.37–5.27	2.44–2.50	1.93–2.77	0.96–1.38
Hydrogenation asphaltenes of West Siberia oil	6.41	2.66	3.75	1.85
Asphaltenes and resins of Surgut oil	5.34	1.82	3.52	1.76
Asphaltenes of Kushkul oil	5.2	1.90	3.30	1.65

**Table 7.**  
*The characteristics of the electronic structure of asphaltenes by EPS method.*

The asphaltenes are complex substances that can be found in crude oil, bitumen, and high-boiling hydrocarbon distillates. The asphaltenes are composed mainly of polyaromatic and heterocyclic compounds with traces of vanadium and nickel, which are in porphyrin structures. The electronic structure of asphaltenes has not been researched enough. The aim of research was to define the electronic structure of various asphaltenes. We have used the EPS methods. Some of the results are shown in **Table 7**.

Thus for asphaltenes, IP is in the interval from 4.37 up to 6.41 eV and EA differs from 1.82 to 2.66 eV. The size of energy band gap from 1.93 to 3.85 eV indicates that oil asphaltenes belong to amorphous, compensated, wideband semiconductors. The experiments for band gap estimation of the asphaltene molecules were confirmed by electronic structure computing with ab initio methods. The main deduction from this research is that oil asphaltenes can be used as organic semiconductors.

**4. Effects of dependence of ionization potentials and electron affinity with color characteristics**

The research [7] (co-author Dr. Shulyakovskaya D. and Dr. Yarmuhametova G.) established the phenomenon of the relationship between the energy of the molecular orbital, which characterizes the IP and EA, and color properties.

$$E = \beta_1 + \beta_2 \cdot q, \tag{25}$$

where E is energy of the boundary molecular orbital (IP or EA), eV;  $\alpha_1$  and  $\alpha_2$  are empirically determined coefficients eV; q is one of the color characteristics (CCs) for standard light source A, B, C, or D; and CCs can be represented in one of the international color measurement systems (e.g., color coordinates or chromaticity coordinates in XYZ or RGB systems). The color coordinates of polycyclic aromatic hydrocarbons in the XYZ system are shown (**Figure 6**). These coordinates are calculated in the visible region of the transmission spectra of hydrocarbon solutions according to the formulas (2)–(7).

Several classes of compounds, including PAH, were studied by dependence (25). The corresponding coefficients for IP and EA are presented in **Tables 8** and **9**. As can be seen from the tables, the accuracy of the assessment of ionization potentials and electron affinity is satisfactory. Thus, the effect of the relationship between IP and EA on the color characteristics can be used to simultaneously measure these physical quantities.

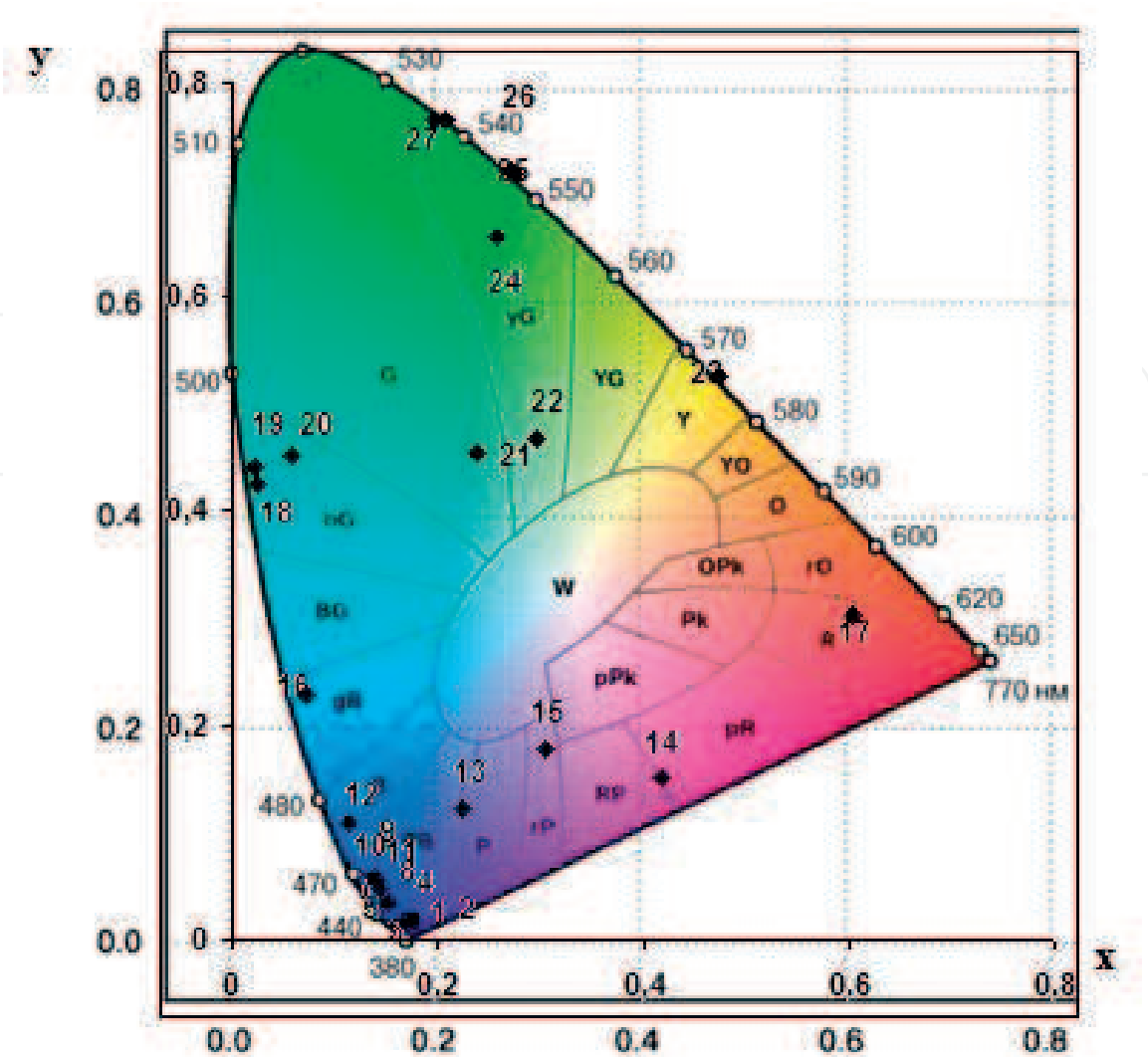


**Figure 6.** Color characteristics (chromaticity coordinates  $x$  and  $y$ ) of the individual aromatic oil components in XYZ colorimetric system: (1) perylene, (2) tetrabenzpentacene, (3) dibenzpyrene, (4) hexabenzcoronene, (5) 1,2-benzphenantrenopyrene, (6) 2,3-benzperylene, (7) dibenzpentacene, (8) phenantrenopyrene, (9) ovalen, (10)–(12) dibenzperylenes, (13) dibenzpyrene, (14) dinaphthpyrene, (15) tetrabenzheptacene, (16) benzanathtpyrene, (17) dibenzanthanthrene, (18) bisantene, (19) benzanathtpyrene, (20) benzbisantene, (21) dinathteptacene, (22) 1, 2-benzanaphthpyrene, (23) dibenzperylene, (24) dibenzanthanthrene, (25) benzperylene, (26) dinaphthpyrene, and (27) tetrabenzheptacen.

Organic semiconductor class	CCs	Coefficients for IP		Correlation coefficients	Variation coefficients (%)	Standard deviation (eV)
		$A_1$ (eV)	$A_0$ (eV)			
Semiconductors containing three and five linear annelated benzene rings and semiconductors of perylene series	$Z_C$	−0.0120	8.2188	0.90	3.10	0.23
	$Z_D$	−0.0129	8.2035	0.89	3.13	0.23
	$B_C$	−0.0023	8.2256	0.89	3.17	0.24
	$B_D$	−0.0024	8.2110	0.89	3.20	0.24
Semiconductor of bisantene series and anthanthrene	$z_C$	4.7985	3.7638	0.94	4.44	0.31
	$z_D$	4.5947	3.9328	0.94	4.47	0.31
	$b_B$	4.2833	3.4563	0.94	4.71	0.32
	$b_C$	5.3597	2.4476	0.94	4.52	0.31
Semiconductors of pyrene series	$x_C$	−4.2636	7.8232	0.87	2.85	0.20
	$x_D$	−4.2503	7.8231	0.86	2.88	0.20

Organic semiconductor class	CCs	Coefficients for IP		Correlation coefficients	Variation coefficients (%)	Standard deviation (eV)
		A <sub>1</sub> (eV)	A <sub>0</sub> (eV)			
Heterocyclic semiconductors	R <sub>A</sub>	−0.0110	7.2866	0.87	2.86	0.20
	R <sub>B</sub>	−0.0148	7.3764	0.87	2.80	0.20
	y <sub>C</sub>	−1.9421	7.7117	0.94	1.92	0.14
	y <sub>D</sub>	−1.8822	7.7100	0.93	1.96	0.14
	g <sub>A</sub>	−1.1612	7.5854	0.91	2.32	0.17
	g <sub>B</sub>	−1.2637	7.5599	0.90	2.41	0.18

**Table 8.**  
*Coefficients of dependence (25) for IP by PAH [4, 7].*

Organic semiconductor class	CCs	Coefficients (25) for EA		Correlation coefficients	Variation coefficients (%)	Standard deviation (eV)	Sample volume (pcs)
		B <sub>1</sub> (eV)	B <sub>0</sub> (eV)				
Semiconductors containing three and five linear annelated benzene rings and semiconductors of perylene series	Z <sub>C</sub>	0.0049	0.6344	0.90	9.92	0.09	29
	Z <sub>D</sub>	0.0053	0.6407	0.89	10.01	0.10	
	B <sub>C</sub>	0.0009	0.6316	0.89	10.77	0.10	
	B <sub>D</sub>	0.0010	0.6376	0.89	10.88	0.10	
Semiconductor of bisantene series and anthanthrene	z <sub>C</sub>	−1.9716	2.4650	0.94	10.65	0.13	11
	z <sub>D</sub>	−1.8879	2.3955	0.94	10.71	0.13	
	b <sub>B</sub>	−1.7597	2.5912	0.94	11.29	0.13	
	b <sub>C</sub>	−2.2019	3.0056	0.94	10.85	0.13	
Semiconductors of pyrene series	x <sub>C</sub>	1.7519	0.7970	0.87	7.62	0.08	20
	x <sub>D</sub>	1.7464	0.7970	0.86	7.68	0.08	
	R <sub>A</sub>	0.0045	1.0175	0.87	7.64	0.08	
	R <sub>B</sub>	0.0061	0.9806	0.87	7.49	0.08	
Heterocyclic semiconductors	y <sub>C</sub>	0.7978	0.8430	0.94	5.71	0.06	15
	y <sub>D</sub>	0.7732	0.8437	0.93	5.82	0.06	
	g <sub>A</sub>	0.4769	0.8949	0.91	6.89	0.07	
	g <sub>B</sub>	0.5190	0.9054	0.90	7.17	0.07	

**Table 9.**  
*Coefficients of dependence (25) for EA by PAH [4, 7].*

The dependence of the IP on the chromatic coordinate-Z in the XYZ system for PAH based on three and five linear annular benzene rings and from the perilene series is shown in **Figure 7**.

The IP and EA values for various organic molecules obtained by the dependence (11) are confirmed by various modifications of quantum DFT and ab initio methods. In addition, the values of IP were estimated by photoelectron spectroscopy. The results are shown in **Tables 10** and **11**.

From the received results, it follows that the equation is distributed to substances with IP < 9.8 eV, i.e., it covers the majority of organic substances.

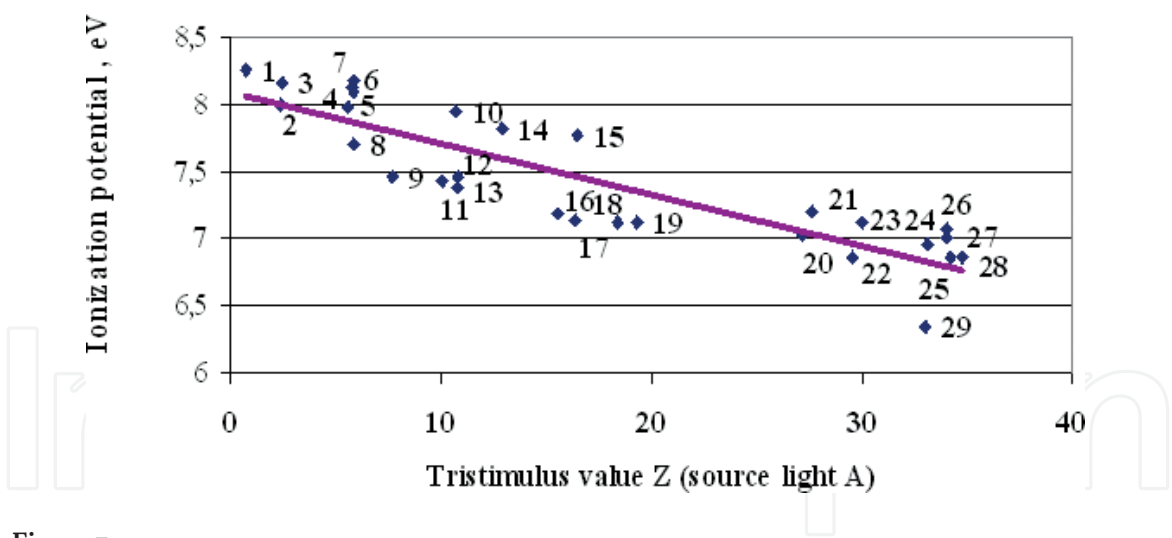


**Figure 7.** The correlation of the first PI and the color characteristic for the compounds with three and five linear annular benzene rings and from the perilene series. (1) 2,3-benzpicene, (2) 1,12-2,3-8,9-tribenzperylene, (3) 1,12-2,3-dibenzperylene; (4) anthracene [2',1':1,2] anthracene; (5) coronene; (6) 2,3-8, 9-dibenzpicene; (7) 3,4-benzpentaphene; (8) pentaphene; (9) perilene; (10) naphtha[2', 3':3, 4]pentaphene; (11) 1,12-o-phenylenperilene; (12) 1,2-benzcoronene; (13) 1,2-3,4-5,6-10,11-tetrabenzanthracene; (14) 2,3-8,9-dibenzpicene; (15) 1,2-7,8-dibenzcoronene; (16) 1,12-o-phenyl-2,3-10,11-dibenzperilene; (17) naphtha [2', 3':1, 2] coronene; (18) 2,3-10, 11-dibenzperylene; (19) 2,3-benzperylene; (20) 1,2-3,4-5,6-tribenzcoronene; (21) anthracene [2', 1',1, 2]tetraphene; (22) 1,2-benzperylene; (23) 1,2-10,11-dibenzperylene; (24) 1,2-3,4-8,9-10,11-tetrabenzpentazene; (25) 1,2-11,12-dibenzperylene; (26) 1,2-8,9-dibenzpentazene; (27) 1,2-benzpentazene; (28) pentazene; and (29) 1,2-7,8-dibenzpicene.

Organic semiconductor class	Semiconductor name	Electron affinity, eV		Abs. accuracy, eV	Rel. accuracy, %
		Regular methods	Acc. to CCs		
Semiconductors containing three and five linear annelated benzene rings and semiconductors of perylene series	Pentaphene	0.85	0.78	0.07	8.24
	Anthraceno [2',1':1,2]anthracene	0.73	0.77	0.04	5.75
	2,3-Benzpicene	0.62	0.70	0.08	12.81
	Anthraceno [2',1':1,2]tetraphene	1.05	1.12	0.06	6.05
	Pentacene	1.19	1.23	0.04	3.36
	1,2-Benzpentacene	1.13	1.22	0.09	7.71
	1,2-3,4-8-9-10,11-Tetrabenzpentacene	1.16	1.20	0.05	4.23
	1,2-Benzperylene	1.19	1.15	0.04	3.55
	1,2-10.11-Dibenzperylene	1.09	1.16	0.07	6.36
	1,2-11.12-Dibenzperylene	1.19	1.22	0.03	2.59
	1,12-2,3-Dibenzperylene	0.66	0.72	0.06	9.75
	1,12-2,3-8,9-Tribenzperylene	0.73	0.72	0.01	0.92
	1,2-3,4-5,6-Tribenzcoronene	1.12	1.11	0.01	1.13

Organic semiconductor class	Semiconductor name	Electron affinity, eV		Abs. accuracy, eV	Rel. accuracy, %
		Regular methods	Acc. to CCs		
Semiconductor of bisantene series and anthanthrene	Bisantene	1.69	1.71	0.02	1.33
	1,14-Benzbisantene	1.11	1.18	0.07	6.32
	3,4-11,12-Dibenzbisantene	0.88	0.93	0.05	5.44
	3,4-10,11-Dibenzbisantene	0.99	0.95	0.04	4.27
	1,2-3,4-8,9-10,11-Tetrabenzbisantene	0.89	0.97	0.08	9.03
	Anthanthrene	1.04	0.92	0.12	11.64
	1,2-7,8-Dibenzanthanthrene	0.95	0.95	0.00	0.02
Semiconductors of pyrene series	3,4-8,9-Dibenzpyrene	1.08	1.03	0.04	3.91
	3,4-9,10-Dibenzpyrene	1.01	1.02	0.02	1.59
	3,4-Benzanaft [2'',3'':8,9]pyrene	1.02	1.02	0.00	0.36
	3,4-Benzanaft [2'',3'':9,10]pyrene	0.97	1.03	0.06	5.93
	Dinaft[2',3':3,4]-[2'',3'':9,10]pyrene	1.00	1.01	0.01	0.97
	1,14-4,5-Dibenzpetacene	1.10	1.04	0.07	6.02
	5,6-15,16-Dibenzhexacene	1.06	1.04	0.03	2.65
	Naft[1',7':2,16]hexacene	1.40	1.40	0.00	0.16
	1,18-4,5-9,10-13,14-Tetrabenzheptacene	1.02	1.02	0.00	0.15
	9-Anthracentiol	0.91	0.93	0.02	2.38
	2,2';5',2''-Tertienil	0.83	0.87	0.05	5.46
	2-Tiapyranthion	1.26	1.30	0.04	3.22
	1,3-Ditiolene-2-thione	0.83	0.90	0.07	8.78
Heterocyclic semiconductors	4,5-Cyclohexeceno-1,3-ditiolene-2-thione	0.85	0.91	0.06	7.26
	4-Phenyl-1,3-ditiolene-2-thione	0.94	0.90	0.04	4.23
	Nafto[1,2-b]-1,3-ditiolene-2-thione	0.97	0.90	0.07	7.48
	4,5-Cyclopenteno-1,2-ditiolene-3-thione	1.18	1.12	0.06	5.12



Organic semiconductor class	Semiconductor name	Electron affinity, eV		Abs. accuracy, eV	Rel. accuracy, %
		Regular methods	Acc. to CCs		
	4,5-Cyclohexeceno-1,2-dithiolene-3-thione	1.12	1.12	0.00	0.21
	4,5-Cyclohepteno-1,2-dithiolene-3-thione	1.18	1.13	0.06	4.75
	Thiolane-3,4-dithion	1.01	1.00	0.01	1.47

**Table 10.**  
*Results of determining electron affinity of some organic semiconductors [7].*

Organic semiconductor class	Semiconductor name	Ionization potential, eV		Abs. accuracy, eV	Rel. accuracy, %
		Regular methods	Acc. to CCs		
Semiconductors containing three and five linear annelated benzene rings and semiconductors of perylene series	Pentaphene	7.70	7.87	0.17	2.22
	Anthraceno [2',1':1,2]anthracene	7.99	7.88	0.10	1.26
	2,3-Benzpicene	8.26	8.07	0.19	2.34
	Anthraceno [2',1':1,2]tetraphene	7.20	7.04	0.15	2.14
	Pentacene	6.87	6.77	0.10	1.41
	1,2-Benzpentacene	7.01	6.80	0.21	3.01
	1,2-3,4-8,9-10,11-Tetrabenzpentacene	6.95	6.83	0.12	1.72
	1,2-Benzperylene	6.87	6.97	0.10	1.48
	1,2-10,11-Dibenzperylene	7.12	6.95	0.17	2.38
	1,2-11,12-Dibenzperylene	6.87	6.79	0.08	1.10
	1,12-2,3-Dibenzperylene	8.16	8.00	0.16	1.92
	1,12-2,3-8,9-Tribenzperylene	7.99	8.00	0.02	0.20
	1,2-3,4-5,6-Tribenzcoronene	7.03	7.06	0.03	0.42
Semiconductor of bisantene series and anthanthrene	Bisantene	5.66	5.60	0.05	0.96
	1,14-benzbisantene	7.06	6.89	0.17	2.42
	3,4-11,12-Dibenzbisantene	7.61	7.50	0.12	1.53
	3,4-10.11-Dibenzbisantene	7.35	7.46	0.10	1.40

Organic semiconductor class	Semiconductor name	Ionization potential, eV		Abs. accuracy, eV	Rel. accuracy, %
		Regular methods	Acc. to CCs		
	1,2-3,4-8,9-10,11-Tetrabenzbisantene	7.60	7.41	0.19	2.56
	Anthanthrene	7.24	7.53	0.29	4.06
	1,2-7,8-Dibenzanthanthrene	7.46	7.46	0.00	0.02
Semiconductors of pyrene series	3,4-8,9-Dibenzpyrene	7.14	7.25	0.10	1.44
Semiconductors of pyrene series	3,4-8,9-Dibenzpyrene	7.14	7.25	0.10	1.44
	3,4-9,10-Dibenzpyrene	7.32	7.28	0.04	0.54
	3,4-Benzanaft [2'',3'':8,9]pyrene	7.29	7.28	0.01	0.13
	3,4-Benzanaft [2'',3'':9,10]pyrene	7.40	7.25	0.14	1.90
	Dinaft[2',3':3,4]-[2'',3'':9,10]pyrene	7.33	7.31	0.02	0.32
	1,14-4,5-Dibenzpetacene	7.08	7.24	0.16	2.28
	5,6-15,16-Dibenzhexacene	7.17	7.24	0.07	0.98
	Naft[1',7':2,16]hexacene	6.35	6.36	0.01	0.10
	1,18-4,5-9,10-13,14-Tetrabenzheptacene	7.29	7.28	0.00	0.07
	9-Anthracentiol	7.54	7.49	0.05	0.71
Heterocyclic semiconductors	2,2';5',2''-Tertienil	7.75	7.64	0.11	1.40
	2-Tiapyranthion	6.69	6.60	0.10	1.46
	1,3-Ditiolene-2-thione	7.76	7.58	0.18	2.27
	4,5-Cyclohexeceno-1,3-ditiolene-2-thione	7.69	7.54	0.15	1.95
	4-Phenyl-1,3-ditiolene-2-thione	7.48	7.58	0.10	1.29

**Table 11.**  
*Results of determining of the first ionization potentials of some organic semiconductors [7].*

Thus, it can be concluded that the effects (21)–(25) discovered by us allow us to estimate the energy levels of quantum systems with sufficient accuracy. This is important for the study of multi-electron systems in molecular electronics and nanotechnology and chemistry such as single molecules, atomic clusters, and high-molecular systems. From here it follows that electronic spectra and color characteristics can be applied to the definition of various characteristics of substances.

## 5. Normal and pathological color characteristics of human blood components

This cycle of works is described [22–26] and executed together with Dr. N. Kalashchenko and Dr. S. Dezortsev. The experiments were conducted at the Ufa Medical University and the Republican Clinic named after Kuvatov (Ufa, Russia).

Colorimetric studies of blood are actively used in medicine [31], criminal law [32], and the food industry [33, 34]. In medical practice, colorimetric methods are used to determine the hemoglobin concentration in the blood of a patient (the color index) [35]. Today a rather exact ( $\pm 1\%$ ) cyanomethemoglobin photometric method is used everywhere, in which cyanomethemoglobin is determined at a wavelength of 540 nm after preparation of a working solution of the blood in Drabkin reagent. Various modifications of this method do not change its essential physical nature [6]. Furthermore, spectral analysis in the visible region has been used to determine oxyhemoglobin and other hemoglobin-containing compounds from the absorption spectra of blood and its solutions [36]. Despite this, the quantitative colorimetric characteristics of blood have not been studied before.

The aim of this work was to study the color characteristics of hemolyzed blood, plasma, and serum from donors in the visible range of the absorption spectra by standard CIE methods (International Commission on Illumination, 1964).

The basic color characteristics (lightness and chromaticity coordinates) determine the position of the color of the specimen in an arbitrary color space and are found by the CIE method [11, 12].

The familiar spectrophotometric method for color measurements involves measuring the spectral power distribution of the radiation followed by calculation of the color coordinates by multiplying the determined spectral power distribution function times the three color-matching functions and then integrating the products. For the spectral power distribution function of the source  $E(\lambda)$ , the spectral transmittance function  $\tau(\lambda)$ , and  $x(\lambda)$ ,  $y(\lambda)$ , and  $z(\lambda)$  (the color-matching functions) and the color coordinates  $X$ ,  $Y$ , and  $Z$  are determined by integration over the wavelength range for visible radiation 380–760 nm. In practice, integration is replaced by summation over the interval  $d\lambda$  (from 5 to 10 nm), since the spectral functions under the integral sign are usually not easily integrated:

$$\begin{aligned} X &= \Delta\lambda \sum_{\lambda} E(\lambda)\tau(\lambda)\bar{x}(\lambda) \\ Y &= \Delta\lambda \sum_{\lambda} E(\lambda)\tau(\lambda)\bar{y}(\lambda), \\ Z &= \Delta\lambda \sum_{\lambda} E(\lambda)\tau(\lambda)\bar{z}(\lambda) \end{aligned} \quad (26)$$

The spectral power distribution and the spectral transmittance curve are measured by separating light into a spectrum, such as in a spectrophotometer or monochromator. The color-matching curves are specified as tables of values of the specific coordinates in 10 nm steps. There are also tables of  $E(\lambda)x(\lambda)$  values for standard CIE light sources A, B, C, and D, characterizing the most typical natural (B, C, D) and artificial (A) illumination conditions.

The chromaticity coordinates are calculated using the formulas.

$$x = \frac{X}{X + Y + Z}, y = \frac{Y}{X + Y + Z}, z = \frac{Z}{X + Y + Z}, x + y + z = 1 \quad (27)$$

The coordinate  $Y$  characterizes the lightness (luminance) of the specimens.

The quantitative colorimetric characteristics of hemolyzed blood, plasma, and serum described by formulas (26) and (27) in the standard CIE method are connected with the transmittance or reflectance spectra and are integrated parameters determined over the entire visible region of the electromagnetic spectrum. So it is assumed that they carry information about the condition of the entire body. In our approach, blood and its components are considered as a single, indivisible light-absorbing system.

The experiment. The objects of investigation were solutions of hemolyzed blood and solutions of plasma and serum (prepared from that blood) of the same concentration from 100 male and female donors (in different blood groups and age groups) and from 95 patients who were assigned to three arbitrary groups: (I) 41 patients with purulent diseases (osteomyelitis, purulent fistulas, gonitis), (II) 41 resuscitated patients (acute myocardial infarction, acute cerebral circulatory collapse, chronic cardiac insufficiency), and (III) 13 patients with cirrhosis of the liver. We determined the color characteristics of the “average” donor (without separating the donors according to blood, sex, and age groups) and compared them with the analogous characteristics of patients from the different groups. The blood for the studies was drawn at a blood donation center and in clinical departments by standard procedures [37].

The spectra of the solutions of hemolyzed blood, plasma, and serum of concentration 2.5 vol.% (1.40) were taken in quartz cuvettes with thickness of the working layer of liquid equal to 10 mm at room temperature, on an SF-2000 spectrophotometer in the range 200–1000 nm in 20 nm steps. As the solvent and the reference solution, we used distilled water for injection, which is optically neutral under the experimental conditions and is the natural physiological solvent in the human body. The hemolyzed blood was prepared using a standard heparin solution, and the plasma was prepared using the preservative Glyugitsir.

In addition to the averaged values of the color coordinates and the lightness value, we calculated the standard deviation, the confidence interval for significance level  $\alpha = 95\%$ , and the coefficient of variation.

**Figure 8** shows the averaged spectra for the hemolyzed blood, plasma, and serum from the patients in all three examined groups compared with the corresponding averaged spectra of the donors. There are clear differences between the different groups of patients.

For the plasma and serum, over the entire studied region, the group spectra for the patients lie higher than the averaged spectra of the donors, and their positional order is consistent: the averaged spectrum for patients with purulent diseases lies above the averaged spectrum for the donors, the averaged spectrum for the

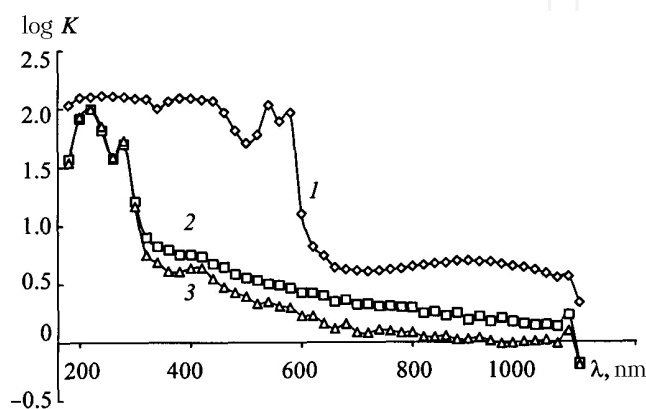


**Figure 8.**  
*Spectra of hemolyzed donor blood (1), plasma (2), and serum (3) in the UV and visible regions (averaged over 100 donors).*

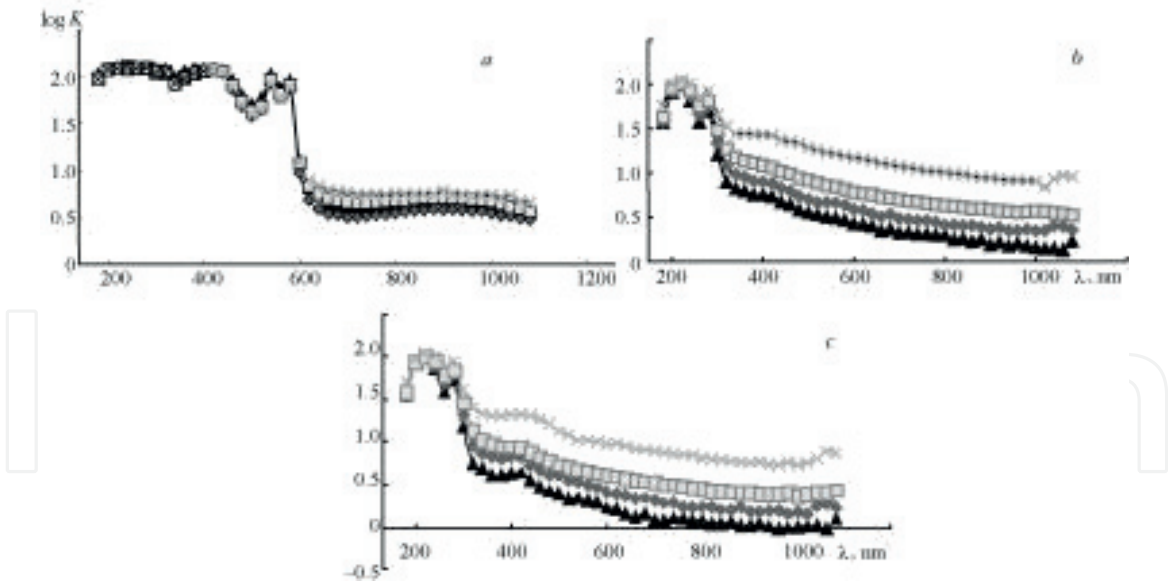


**Figure 9.** Averaged spectra of hemolyzed blood (a), plasma (b), and serum (c) of examined groups of patients ( $\blacktriangle$  = donors,  $\triangle$  = I,  $\square$  = II,  $\times$  = III) compared with averaged spectrum of hemolyzed blood, plasma, and serum, respectively, from donors [25].

resuscitation patients lies above that spectrum, and the averaged spectrum for patients with cirrhosis of the liver lies even higher. Probably such positioning of the spectra reflects the severity of the general condition of the patients, if we assume that cirrhosis is the most severe condition for the patients with the least likelihood of recovery. We do not observe such a dependence for the hemolyzed blood: the averaged spectrum for the patients with purulent diseases lies below the averaged spectrum for the donors (**Figure 9**).

**Table 12** gives the averaged color coordinates and lightness for the donors and each group of examined patients, calculated for the solutions of blood, plasma, and serum as a single light-absorbing system according to the standard CIE method. For the donors, the chromaticity coordinate  $x$  varies from  $0.320 \pm 0.001$  (for serum and plasma) to  $0.630 \pm 0.008$  (for hemolyzed blood). The coefficients of variation in this case also decrease from 4.7 for blood down to 1.3 for serum. The chromaticity coordinate  $y$  for the donors has similar values:  $0.320 \pm 0.002$  for plasma and serum and  $0.340 \pm 0.003$  for blood. The coefficients of variation for  $y$  steadily decrease from 3.2 for blood down to 2.0 for serum. The parameter  $z$  for the donors is higher for serum and plasma ( $0.360 \pm 0.003$ ) than for blood ( $0.030 \pm 0.005$ ). The coefficient of variation for this parameter is maximum for blood (67.6) and minimum for serum (2.5). The lightness, as expected, has the maximum value (84.88–1.54) for serum and the minimum value (11.55–0.67) for hemolyzed blood. For plasma, this parameter is close to the value typical of serum.

In determining the color range (see **Figure 9a**) for the dilute solutions (1.40) of hemolyzed blood, plasma, and serum from the donors, the color range of blood falls within the red region of the spectrum; the range for plasma and serum falls within the yellow region with lower saturation, which supports the correctness of our experiments and calculations. The corresponding regions for the color range for the patients cover a larger area than for the donors (**Figure 9b**). In order to better visualize the results obtained, we calculated the color coordinates for the studied specimens with correction for concentration. All the points for the donors lie within the yellow-orange region with saturation of 30–50%, which corresponds to the visual observations.

The average values of the color coordinates for all the patient groups (see **Table 12**) are virtually no different from the averages for the donors except for



Parameter	Hemolyzed blood				Plasma				Serum			
	Donors	I	II	III	Donors	I	II	III	Donors	I	II	III
Chromaticity coordinate $x$												
Mean value	0.63	0.59	0.64	0.34	0.32	0.335	0.33	0.35	0.32	0.32	0.32	0.35
Standard deviation	0.029	0.041	0.032	0.048	0.005	0.009	0.013	0.02	0.004	0.009	0.016	0.019
Confidence interval, $\alpha = 0.95$	0.01	0.01	0.01	0.02	0.001	0.002	0.004	0.01	0.001	0.002	0.005	0.009
Coefficient of variation	4.7	6.9	5.46	8.11	1.6	2.65	4.13	5.82	1.3	2.9	4.93	5.5
Chromaticity coordinate $y$												
Mean value	0.34	0.35	0.35	0.36	0.32	0.33	0.34	0.36	0.32	0.33	0.34	0.37
Standard deviation	0.011	0.013	0.011	0.014	0.008	0.011	0.011	0.019	0.006	0.011	0.012	0.019
Confidence interval, $\alpha = 0.95$	0.003	0.003	0.003	0.007	0.002	0.003	0.004	0.009	0.002	0.003	0.004	0.009
Coefficient of variation	3.2	3.67	3.07	3.98	2.6	3.36	3.37	5.27	2.0	3.55	3.61	5.22
Chromaticity coordinate $z$												
Mean value	0.03	0.005	0.05	0.06	0.36	0.34	0.33	0.29	0.36	0.35	0.34	0.29
Standard deviation	0.02	0.028	0.024	0.034	0.012	0.017	0.024	0.039	0.009	0.019	0.026	0.038
Confidence interval, $\alpha = 0.95$	0.005	0.007	0.008	0.017	0.003	0.004	0.008	0.019	0.003	0.005	0.008	0.019
Coefficient of variation	67.6	53.77	53.16	61.58	3.3	4.98	7.29	13.46	2.5	5.53	7.76	13.26
Lightness $L$ , %												
Mean value	11.55	14.82	12.99	13.46	78.94	67.82	63.04	36.66	84.88	79.34	72.42	48.08
Standard deviation	2.46	3.5	2.72	5.8	8.17	12.42	14.79	19.65	5.58	10.21	16.46	22.77
Confidence interval, $\alpha = 0.95$	0.67	0.9	0.85	2.84	2.19	3.11	4.62	9.63	1.54	2.62	5.14	11.15
Coefficient of variation	21.3	23.86	21.38	43.07	10.3	18.11	23.92	53.6	6.6	13.03	23.2	47.35
<i>*Note: I, II, and III indicate the arbitrary groups of patients.</i>												

**Table 12.**  
*Integrated normal and pathological color characteristics of hemolyzed human blood, plasma, and serum [22–25].*

Samples of blood plasma	Patients with liver cirrhosis		Healthy people	
	x	y	x	y
1	0.348	0.350	0.322	0.324
2	0.345	0.348	0.324	0.326
3	0.341	0.343	0.318	0.315
4	0.383	0.373	0.331	0.325
5	0.348	0.357	0.321	0.315
6	0.339	0.348	0.323	0.317
7	0.360	0.368	0.315	0.316
8	0.350	0.363	0.322	0.326
9	0.372	0.375	0.33	0.331
10	0.342	0.347	0.309	0.31
11	0.344	0.346	0.313	0.311
12	0.359	0.356	0.326	0.325
13	0.345	0.347	0.317	0.318
14	0.357	0.359	0.314	0.317
15	0.353	0.360	0.319	0.325

**Table 13.**  
*The chromaticity coordinates (x and y) of patients with liver cirrhosis and healthy people [25].*

Statistical indicators	Patients with liver cirrhosis		Healthy people	
	x	y	x	y
Mean	0.352	0.356	0.320	0.320
Confidence interval	0.006	0.005	0.001	0.002
Dispersion, $\sigma$	0.02	0.02	0.005	0.008
Error of mean	0.003	0.002	0.001	0.001
Variation coefficient	5.62	4.80	1.6	2.6

**Table 14.**  
*The statistical characteristics of chromaticity coordinates for blood plasma of healthy individuals and patients with liver cirrhosis in the XYZ system [25].*

patients with cirrhosis of the liver, for which the bilirubin blood concentration sharply increases. As a result of this, the plasma and serum take on a saturated orange color, which is reflected in the spectra and accordingly in their color characteristics. For the same reason, the lightness of the plasma and serum for these patients is much lower (by almost a factor of two) than for the rest. However, we do not observe sharp differences in the spectra of the hemolyzed blood.

The lightness of the plasma and serum depends on the condition of the patients. Thus the average values of this parameter for the plasma decrease as the severity of the diseases increases: from 78.94 for the donors up to 67.82 for septic patients, 63.04 for resuscitated patients, and 36.66 for patients with cirrhosis of the liver.

In the future, we performed new experiments in which the possibility of diagnosis of liver cirrhosis by color characteristics of blood was considered [23].

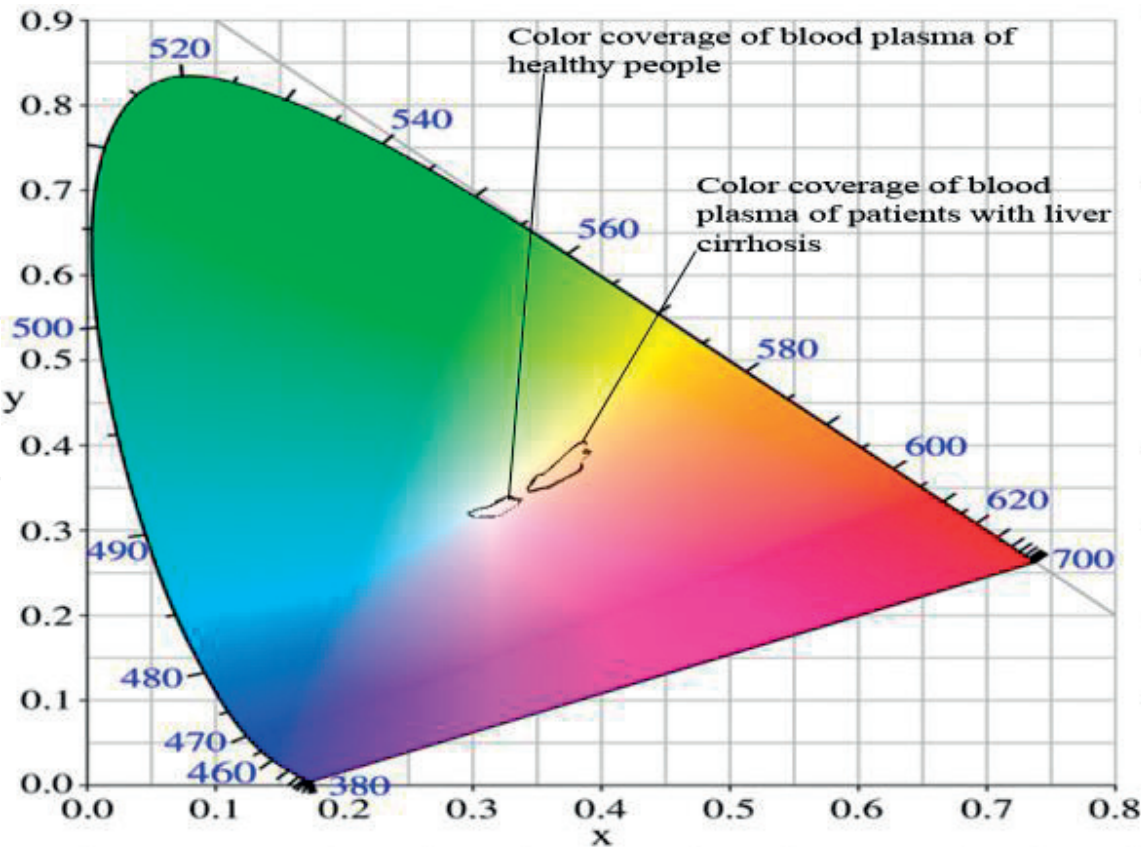


**Figure 10.**  
*Blood plasma of patients with liver cirrhosis and healthy people on the chromaticity diagram of system XYZ (Source C) [24, 25].*

The color characteristics of the samples of blood plasma were calculated after processing spectra. The selective figures of the chromaticity coordinates of patients with liver cirrhosis and healthy people are shown in **Table 13**.

Then the statistical analysis of the data was made. The basic statistics for all the investigated samples are shown in **Table 14**.

Totalities of samples have a distribution close to normal and similar values of dispersion; therefore the t-test can be used to assess the reliability of the results. T of t-test for the chromaticity coordinate x was 10.57, for y—12.9. The critical value of t for confidence probability p = 0.999 is 3.5, which is much smaller than the obtained results. Consequently, the differences between chromaticity coordinates of groups of patients and donors were statistically significant.

The differences between the color characteristics of blood plasma of patients with liver cirrhosis and healthy subjects are shown in **Figure 10**.

Colorimetric method established that a healthy person is characterized by the following indicators of chromaticity coordinates:

$$x = 0.32 \pm 0.001, y = 0.32 \pm 0.002.$$

Patients with liver cirrhosis are characterized by the following color characteristics:  $x = 0.352 \pm 0.006$   $y = 0.356 \pm 0.005$ .

Having made the statistical processing, the data revealed that color characteristics of blood plasma of patients with liver cirrhosis differ from color characteristics of blood plasma of healthy people with a high degree of reliability.

Investigation of human blood plasma by colorimetric methods can be used to express diagnosis of liver cirrhosis. A healthy person is characterized by the following indicators of chromaticity coordinates:  $x = 0.32 \pm 0.001$ ,  $a = 0.32 \pm 0.002$ .

Patients with cirrhosis of the liver are *characterized by the following color* characteristics:  $x = 0.352 \pm 0.006$   $a = 0.356 \pm 0.005$ .

Hence based on the integrated absorption spectra according to the standard CIE system, using the absorption coefficient for radiation in the visible wavelength range, we quantitatively determined the normal and pathological average color characteristics of human blood and its components (plasma and serum). The condition of the body is most adequately described using the lightness parameter for the aqueous solutions of plasma and serum. The method can be used in medical practice for rapid health assessment.


### Author details

Mikhail Dolomatov

Department of Physical Electronics and Nanophysics, Physical and Technical Institute, Bashkir State University, Ufa, Bashkortostan Republic, Russia

\*Address all correspondence to: [mdolomatov@bk.ru](mailto:mdolomatov@bk.ru)

### IntechOpen

© 2019 The Author(s). Licensee IntechOpen. This chapter is distributed under the terms of the Creative Commons Attribution License (<http://creativecommons.org/licenses/by/3.0>), which permits unrestricted use, distribution, and reproduction in any medium, provided the original work is properly cited. 

## References

- [1] Bensaude-Vincent B, Stengers I. A History of Chemistry. Cambridge, MA and London: Harvard University Press; 1997. 305 p. ISBN: 0-674-39659-6
- [2] Dolomatov MY. Some physico-chemical aspects of prediction properties of multicomponent systems in conditions of extreme influences. Journal of D.I. Mendeleev Russian Chemical Society. 1990;**36**(5):632-639
- [3] Dolomatov MY. Fragments of Real Substance Theory, From Hydrocarbon Systems to Galaxies. Moscow: Chemistry; 2005. p. 208. ISBN: 5-98109-018-9
- [4] Dolomatov MY, Mukaeva GR, Shulyakovskaya DO. Electron phenomenological spectroscopy and its application in investigating complex substances in chemistry, nanotechnology and medicine. Journal of Materials Science and Engineering B. 2013;**3**(3):183-199
- [5] Dolomatov MY, Kydyrgychova OT, Dolomatova LA, Kartasheva VV. Color the characteristics petrochemical systems. Journal of Applied Spectroscopy. 2000;**67**(3):536-540
- [6] Dolomatov MY, Yarmukhametova GU. Correlation of color characteristics with conradson carbon residue and molecular weight of complex hydrocarbon media. Journal of Applied Spectroscopy. 2008;**75**(3):433-438
- [7] Dolomatov MY, Jarmuhametova GU, Dolomatova LA. The interaction of color and physicochemical properties of hydrocarbon systems in colorimetric systems RGB and XYZ. Journal of Applied Physics. 2008;**4**:43-49. (Russia)
- [8] Dolomatov MY, Shulyakovskaya DO, Yarmukhametova GU, Mukaeva GR. Evaluation of physico-chemical properties of hydrocarbon systems based on spectrum-property and color-property correlations. Chemistry and Technology of Fuels and Oils. 2013;**49**(3):273-280
- [9] Dolomatov MY, Jarmuhametova GU. Number-average molecular weight definition of oils and petroleum residues by color characteristics. Chemistry and Technology Fuels and Oils. 2009;**4**: 46-49
- [10] Dolomatov MY, Jarmuhametova GU. Calculation of average molecular mass, cocking capacity and viscous flow activation energy of oil surface samples by color-properties correlations. Geology, Geophysics and Reservoir Engineering. 2009;**7**:35-38. (Russia)
- [11] ISO/CIE 10526. CIE standard illuminants for colorimetry
- [12] Fairchild MD. Color Appearance Models. 2nd ed. Chichester, UK: Wiley-IS & T Series in Imaging Science and Technology; 2005
- [13] The directory "Methods of research in textile chemistry". G.E. Krichevskii ed. Moscow: Lights industrial publishers; 1993
- [14] Dolomatov MY, Mukaeva GR. Method for determining the ionization potential and electron affinity of atoms and molecules using electron spectroscopy. Journal of Applied Spectroscopy. 1992;**56**(4):344-347
- [15] Dolomatov MY, Shulyakovskaya DO, Mukaeva GR, Jarmuhametova GU, Latypov KF. Simple characteristics estimation methods of material and molecule electronic structure. Journal of Materials Science and Engineering B. 2012;**(4)**:261-268
- [16] Dolomatov MY, Jarmuhametova GU, Shulyakovskaya DO. The estimation of the first ionization



potentials and electron affinity of the molecules of polycyclic organic semiconductors applying the color characteristics in colorimetric systems XYZ and RGB. *Journal of Applied Physics*. 2011;1:20-31. (Russia)

[17] Dolomatov MY, Shulyakovskaya DO, Mukaeva GR, Paymurzina NK. Testing amorphous, multi-component, organic dielectrics according to their electronic spectrums and color characteristics. *Applied Physics Research*. 2012;3:83-87

[18] Dolomatov MY, Mukaeva GR, Jarmuhametova GU, Shulyakovskaya DO. Simple definition methods of electron structures of materials and molecules for nanoelectronics. *Nanotech Europe*, Berlin, Germany; 2009. pp. 172. Available from: <http://www.nanotech.net/content/conference/abstract-submission/simple-definition-methods-electron-structures-materials-and-m>

[19] Dolomatov MY, Paymurzina NK, Latypov KF, Kovaleva EA. Specific quantum effects in atomic and molecular systems. *Journal of Materials Science and Engineering A*. 2013;3(12): 183-190

[20] Dolomatov MY, Kovaleva EA, Paymurzina NH. Phenomenological approach to mathematical analysis of the electron spectra of organic semiconductors. *Journal Nanotechnology: Development and Applications—XXI Century*. 2016;8(4): 43-48. (In Russian)

[21] Dolomatov MY, Latypov KF. Determination of heterocyclic molecules ionization potential based on optical absorption spectra of electromagnetic radiation in the visible and UV range. *Fotonika (Photonika)*. 2017;4:60-67. (In Russian)

[22] Dolomatov MY, Kalashchenko NV, Dezortsev SV, Araslanov TR. Features

of color characteristics of blood plasma of patients with liver cirrhosis in the colorimetric system XYZ as compared with healthy people. *International Journal of Clinical Medicine*. 2012;3(3): 211-214

[23] Dolomatov MY, Kalashchenko NV, Arslanov TR, Dezortsev SV. Spectroscopic phenomenological estimation of the functional state of human organism in rate and pathology. *International Journal of Clinical Medicine*. 2011;2:79-81

[24] Kalashchenko NV, Dolomatov MY, Dezortsev SV. *The Electronic Phenomenological Spectroscopy Blood of Human in Rate and Pathology, Theory and Practice Aspects*. Moscow: Inter; 2010. p. 256. ISBN: 978-5-98761-034-3

[25] Kalashchenko NW, Dolomatov MY, Dezortsev SV, Popova EA, Kurmankaeva RR. Normal and pathological color characteristics of human blood components. *Journal of Applied Spectroscopy*. 2006;3:220-225

[26] Dolomatova LA, Kalashchenko NV, Dezortsev SN, Dolomatov MY. Definition of level of persons health on color features of the biological liquids in RGB colorimetric system. *Journal Biomedical Radio Electronics*. 2009;(6): 10-13

[27] Wales DJ, editor. *Intermolecular Forces and Clusters*. Vol. 1. New York: Springer Berlin Heidelberg; 2005

[28] Jensen F. *Introduction to Computational Chemistry*. John Wiley & Sons; 2007. 599 p

[29] Tikhonov VI. *Statistical Radiotechnics*. Moscow: Radio i svyaz' Publ; 1982. 624 p. (In Russian)

[30] Dolomatov MY, Petrov AM, Bakhtizin RZ, et al. Asphaltenes as new objects for nanoelectronics. *IOP*

Conference Series: Materials Science  
and Engineering. 2017;**195**:29-32

[31] Kamyshnikov VS. Clinical  
Biochemical Laboratory Diagnostics:  
Handbook (in Russian). Interpresservis.  
Vols. 1 and 2. Minsk; 2003

[32] Barsegyants LO. Forensic Medical  
Investigation of Material Evidence (in  
Russian). Moscow: Meditsina; 1999

[33] Kudryashov LS, Gurinovich GV,  
Potipaeva NN. Method for meat quality  
control. Russian Federation Patent No.  
2092836; 1997

[34] Kudryashov LS, Gurinovich GV.  
Molotchnaya Industriya, No. 5 (1998)  
(in Russian). Available from:  
[http://food-machex.mtc.ru/mi/mi\\_05\\_98/topic7.htm](http://food-machex.mtc.ru/mi/mi_05_98/topic7.htm)

[35] Nazarenko GI, Kishkun AA. Clinical  
Assessment of Laboratory Research  
Results (in Russian). Moscow:  
Meditsina; 2000

[36] Pupkova VI. Determination of  
hemoglobin in blood (in Russian).  
Available from: <http://www.vector-best.com/ru/brosh/hemo-glob.htm>

[37] Berezov TT, editor. Laboratory  
Manual for Biological Chemistry (in  
Russian). Moscow: Meditsina; 1976